Inorg. Chem. **2004**, *43*, 6024–6034

Cyclohexene Oxide/CO_2 Copolymerization Catalyzed by Chromium(III) Salen Complexes and *N*-Methylimidazole: Effects of Varying Salen Ligand Substituents and Relative Cocatalyst Loading

Donald. J. Darensbourg,* Ryan M. Mackiewicz, Jody L. Rodgers, Cindy C. Fang, Damon R. Billodeaux, and Joseph H. Reibenspies

Department of Chemistry, Texas A&M University, College Station, Texas 77843

Received June 23, 2004

A detailed mechanistic study into the copolymerization of CO_2 and cyclohexene oxide utilizing Cr^{III}(salen)X complexes and *N*-methylimidazole, where H_2salen = *N*,*N*′-bis(3,5-di-*tert*-butylsalicylidene)-1,2-ethylenediimine and other salen derivatives and X = Cl or N_3, has been conducted. By studying salen ligands with various groups on the diimine backbone, we have observed that bulky groups oriented perpendicular to the salen plane reduce the activity of the catalyst significantly, while such groups oriented parallel to the salen plane do not retard copolymer formation. This is not surprising in that the mechanism for asymmetric ring opening of epoxides was found to occur in a bimetallic fashion, whereas these perpendicularly oriented groups along with the *tert*-butyl groups on the phenolate rings produce considerable steric requirements for the two metal centers to communicate and thus initiate the copolymerization process. It was also observed that altering the substituents on the phenolate rings of the salen ligand had a 2-fold effect, controlling both catalyst solubility as well as electron density around the metal center, producing significant effects on the rate of copolymer formation. This and other data discussed herein have led us to propose a more detailed mechanistic delineation, wherein the rate of copolymerization is dictated by two separate equilibria. The first equilibrium involves the initial second-order epoxide ring opening and is inhibited by excess amounts of cocatalyst. The second equilibrium involves the propagation step and is enhanced by excess cocatalyst. This gives the [cocatalyst] both a positive and negative effect on the overall rate of copolymerization.

Introduction

Carbon dioxide is one of the most abundant, nontoxic, nonflammable, environmentally friendly C_1 feedstocks available.[1] However, because of its high thermodynamic stability it is greatly underutilized. Despite this, one process that has shown significant gains in the past 10 years is the copolymerization of CO_2 and epoxides to provide polycarbonates.[2] This route becomes viable because the energy gained by releasing the ring strain of the three-membered oxirane is significant enough to overcome the energy needed to destabilize the inert CO_2 molecule. Indeed, the reaction depicted in eq 1, specifically involving cyclohexene oxide, is very important since it represents an environmentally benign synthetic route to these biodegradable thermoplastics, otherwise prepared by the interfacial polycondensation of the *trans*-diols and phosgene. A variety of *efficient* catalysts or catalyst precursors for the copolymerization of cyclohexene oxide[3] and carbon dioxide and a few accounts of very active catalysts for the copolymerization of propylene oxide[4] and carbon dioxide have been reported recently.

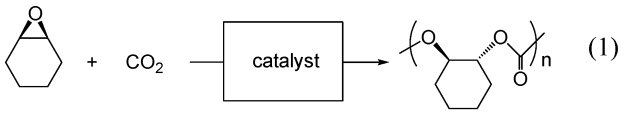

poly(cyclohexylene)carbonate

* Author to whom correspondence should be addressed. E-mail: djdarens@mail.chem.tamu.edu. Fax: (979) 845-0158.

(1) (a) Gibson, D. H. *Chem. Rev.* **1996**, *96*, 2063−2095. (b) Leitner, W. *Coord. Chem. Rev.* **1996**, *155*, 257−284. (c) Yin, X.; Moss, J. R. *Coord. Chem. Rev.* **1999**, *181*, 27−59. (d) Aresta, M., Schloss, J. V., Eds. *Enzymatic and Model Carboxylation and Reduction Reactions for Carbon Monoxide Utilization*; NATO ASI Series No. C314; Kluwer: Dordrecht, The Netherlands, 1990. (e) Brauden, C.-I., Schneider, G., Eds. *Carbon Dioxide Fixation and Reduction in Biological and Model Systems*; Oxford University Press: Oxford, U.K., 1994.

(2) For reviews on epoxide/CO_2 copolymerization processes, see: (a) Darensbourg, D. J.; Holtcamp, M. W. *Coord. Chem. Rev.* **1996**, *153*, 155−174. (b) Beckman, E. *Science* **1999**, *283*, 946−947. (c) Super, M. S.; Beckman, E. *J. Trends Polym. Sci.* **1997**, *5*, 236−240. (d) Rokicki, A.; Kuran, W. *J. Macromol. Sci., Rev. Macromol. Chem. Phys.* **1991**, *C21*, 135−186. (e) Coates, G. W.; Moore, D. R. *Angew. Chem., Int. Ed.*, in press.

10.1021/ic049182e CCC: $27.50
Published on Web 08/10/2004

Chronologically, catalysts derived from zinc have played pivotal roles in the development of this chemistry. These began with the prototypical study of Inoue[5] followed by that of Soga[6] both involving heterogeneous zinc catalysts, to the discrete zinc phenoxide complexes by our group,[7] to the very effective β-diiminate zinc complexes of Coates and co-workers.[8] More recently other metal derivatives are proving to be very efficient at catalyzing the CO_2/epoxide coupling reaction, e.g., chromium porphyrinates,[9] chromium salen,[10] and cobalt salen[4a] complexes. An important feature of these latter derivatives is that they are *extremely robust* catalyst systems. A present focus of our research program is the further development of catalytic systems on the basis of metal salen complexes, with emphasis being placed on in situ monitoring of these processes by infrared spectroscopy in an effort to optimize conditions for the copolymerization of CO_2 with a variety of epoxides.

Although, the salen (*N*,*N*′-bis(salicylidene)-1,2-ethylenediimine) ligand and its derivatives complexed to a range of transition and main group metals have served to catalyze a variety of organic transformations, the work most relevant to this publication is the asymmetric ring-opening (ARO) of epoxides first performed by Jacobsen and co-workers.[11] The high enantomeric excess, outstanding yields, and Jacobsen's proposed bimetallic ring-opening mechanism pioneered many new directions in catalysis. Our initial studies centered on Jacobsen's catalyst, (*N*,*N*′-bis(3,5-di-*tert*-butylsalicylidene)-(1*R*,2*R*)-cyclohexenediimino)chromium chloride, and illustrated the viability of utilizing chromium salen complexes for the copolymerization of CO_2 and epoxides, producing polymer with high carbonate content, >99%, little cyclic carbonate, and a very low polydispersity index (PDI = 1.2).[10a] Herein we wish to report a thorough study of the different aspects of the salen architecture, the effect of varying the amount of cocatalyst, and the type of initiator present at the chromium center on the catalytic efficiency of the CO_2/cyclohexene oxide coupling reaction.

Experimental Section

Methods and Materials. Unless otherwise specified, all syntheses and manipulations were carried out on a double-manifold Schlenk vacuum line under an atmosphere of argon or in an argon-filled glovebox. Benzene, diethyl ether, pentane, tetrahydrofuran, and toluene were freshly distilled from sodium benzophenone ketal. Cyclohexene oxide (Lancaster) and propylene oxide (Aldrich) were freshly distilled from CaH_2. 2-(3,4-Epoxycyclohexyl)ethyltrimethoxysilane was purchased from Gelest and vacuum distilled from CaH_2. *N*-Methylimidazole was purchased from Aldrich and distilled over sodium metal prior to use. Bone dry carbon dioxide supplied in a high-pressure cylinder equipped with a liquid dip-tube was purchased from Scott Specialty Gases. Substituted ethylenediamine precursors for salen ligands **1**−**3** were synthesized by a previously published method.[12] 5-Methoxysalicylaldehyde, KH (Aldrich), 1-methylethylenediamine (TCI Japan), and $AgClO_4$ (Strem) were used without further purification. 3,5-Di-*tert*-butylsalicylaldehyde[13] and 3-*tert*-butyl-5-methoxysalicylaldehyde[14] were synthesized as described in the literature. The following salicylaldimine ligands have been described previously: *N*,*N*′-bis(3,5-di-*tert*-butylsalicylidene)-1-methylethylenediimine (**4**); *N*,*N*′-bis(3,5-di-*tert*-butylsalicylidene)-(±)-1,2-diphenylethylenediimine (**5**);[15] *N*,*N*′-bis(salicylidene)ethylenediimine (**6**);[16] *N*,*N*′-bis(3-*tert*-butyl-5-methoxysalicylidene)ethylenediimine (**10**);[17] *N*,*N*′-bis(salicylidene)phenylenediimine (**11**);[17] *N*,*N*′-bis(3,5-di-*tert*-butylsalicylidene)-(1*R*,2*R*)-cyclohexenediimine (**16**).[14] Details of the synthesis of several of the salen ligands and their corresponding chromium complexes are reported in the Supporting Information. Unless otherwise stated, all other reagents were used without further purification. ^{1}H and ^{13}C NMR spectra were acquired on Unity+ 300 MHz and VXR 300 MHz superconducting NMR spectrometers. The operating frequency for ^{13}C experiments was 75.41 MHz. Infrared spectra were recorded on a Mattson 6021 FT-IR spectrometer with DTGS and MCT detectors. Analytical elemental analysis was provided by Canadian Microanalytical Services Ltd.

Synthesis of *N*,*N*′-Bis(3,5-di-*tert*-butylsalicylidene)-1,2-di-*tert*-butylethylenediimine (1). 1,2-Di-*tert*-butylethylenediamine (4.17 g, 24.2 mmol), 3,5-di-*tert*-butylsalicylaldehyde (11.3 g, 48.3 mmol), and a few drops of aqueous formic acid were dissolved in 100 mL of methanol and heated to reflux for 2 h. Product isolation produced a yellow solid (2.99 g, 20% yield). Crystals suitable for X-ray analysis were grown by slow evaporation of pentane. Anal. Calcd for $C_{40}H_{64}N_2O_2$: C, 79.41; H, 10.66; N, 4.63. Found: C, 78.94; H, 10.62; N, 4.83. ^{1}H NMR (C_6D_6, 300 MHz): δ 14.32 (s, 2H),

(3) (a) Darensbourg, D. J.; Holtcamp, M. W.; Struck, G. E.; Zimmer, M. S.; Niezgoda, S. A.; Rainey, P.; Robertson, J. B.; Draper, J. D.; Reibenspies, J. H. *J. Am. Chem. Soc.* **1999**, *121*, 107−116. (b) Darensbourg, D. J.; Wildeson, J. R.; Yarbrough, J. C.; Reibenspies, J. H. *J. Am. Chem. Soc.* **2000**, *122*, 12487−12496. (c) Cheng, M.; Moore, D. R.; Reczek, J. J.; Chamberlain, B. M.; Lobkovsky, B. E.; Coates, G. W. *J. Am. Chem. Soc.* **2001**, *123*, 8738−8749. (d) Cheng, M.; Darling, N. A.; Lobkovsky, E. B.; Coates, G. W. *Chem. Commun.* **2000**, 2007−2008. (e) Moore, D. R.; Cheng, M.; Lobkovsky, E. B.; Coates, G. W. A*ngew. Chem., Int. Ed.* **2002**, *41*, 2599−2602. (f) Eberhardt, R.; Allmendinger, M.; Luinstra, G. A.; Rieger, B. *Organometallics* **2003**, *22*, 211−214. (g) Moore, D. R.; Cheng, M.; Lobkovsky, E. B.; Coates, G. W. *J. Am. Chem. Soc.* **2003**, *115*, 11911−11924.

(4) (a) Qin, Z.; Thomas, C. M.; Lee, S.; Coates, G. W. *Angew. Chem., Int. Ed.* **2003**, *42*, 5484−5487. (b) Eberhardt, R.; Allmendinger, M.; Rieger, M. *Macromol. Rapid Commun.* **2003**, *24*, 194−196. (c) Darensbourg, D. J.; Mackiewicz, R. M.; Rodgers, J. L.; Phelps, A. L. *Inorg. Chem.* **2004**, *43*, 1831−1833. (d) Lu, X.-B.; Wang, Y. *Angew. Chem., Int. Ed.* **2004**, *43*, 3574−3577.

(5) Inoue, S.; Koinuma, H.; Tsuruta, T. *Polym. Sci., Part B: Polym. Lett.* **1969**, *7*, 287−292.

(6) Soga, K.; Imai, E.; Hattori, I. *Polymer J.* **1981**, *13* (4), 407−410.

(7) Darensbourg, D. J.; Holtcamp, M. W. *Macromolecules* **1995**, *28*, 7577−7579.

(8) Cheng, M.; Lobkovsky, E. B.; Coates, G. W. *J. Am. Chem. Soc.* **1998**, *120*, 11018−11019.

(9) (a) Kruper, W. J.; Dellar, D. V. *J. Org. Chem.* **1995**, *60*, 725−727. (b) Mang, S.; Cooper, A. I.; Colclough, M. E.; Chauhan, N.; Holmes, A. B. *Macromolecules* **2000**, *33*, 303−308. (d) Stamp, L. M.; May, S. A.; Holmes, A. B.; Knights, K. A.; de Miguel, Y. R.; McConvey, I. F. *Chem. Commun.* **2001**, 2502−2503.

(10) (a) Darensbourg, D. J.; Yarbrough, J. C. *J. Am. Chem. Soc.* **2002**, *124*, 6335−6342. (b) Darensbourg, D. J.; Yarbrough, J. C.; Ortiz, C.; Fang, C. C. *J. Am. Chem. Soc.* **2003**, *125*, 7586−7591.

(11) (a) Martinez, L. E.; Leighton, J. L.; Carsten, D. H.; Jacobsen, E. N. *J. Am. Chem. Soc.* **1995**, *117*, 5897−5898. (b) Hansen, K. B.; Leighton, J. L.; Jacobsen, E. N. *J. Am. Chem. Soc.* **1996**, *118*, 10924−10925. (c) Jacobsen, E. N. *Acc. Chem. Res.* **2000**, *33*, 421−431. (d) Nielson, L. P. C.; Stevenson, C. P.; Blackmond, D. G.; Jacobsen, E. N. *J. Am. Chem. Soc.* **2004**, *126*, 1360−1360.

(12) Roland, S.; Mangwnwy, P. *Eur. J. Org. Chem.* **2000**, 611−616.

(13) Casiraghi, G.; Casnati, G.; Puglia, G.; Sartori, G.; Terenghi, G. *J. Chem. Soc., Perkin Trans. 1* **1980**, 1862−1865.

(14) Larrow, J. F.; Jacobsen, E. N. *J. Org. Chem.* **1994**, *59*, 1939−1942.

(15) Zang, W.; Loebach, J. L.; Wilson, S. R.; Jacobsen, E. N. *J. Am. Chem. Soc.* **1990**, *112*, 2801−2803.

(16) Pfeiffer, P.; Breith, E.; Lubbe, E.; Tsumaki, T. *Liebigs Ann.* **1933**, *503*, 84.

(17) Nishinaga, A.; Tsutsui, T.; Moriyama, H.; Wazaki, T.; Mashino, T.; Fujii, Y. *J. Mol. Catal.* **1993**, *83*, 117−123.

8.23 (s, 2H), 7.62 (d, $J = 2.4$ Hz, 2H), 7.21 (d, $J = 2.4$ Hz, 2H), 3.17 (s, 2H), 1.70 (s, 18H), 1.36 (s, 18H), 0.77 (s, 18H). $^{13}C\{^1H\}$ NMR (C_6D_6, 75 MHz): δ 167.32, 159.97, 140.26, 138.07, 127.78, 126.51, 118.80, 78.17, 36.37, 35.97, 34.67, 32.13, 30.29, 28.19.

Synthesis of *N*,*N*′-Bis(3,5-di-*tert*-butylsalicylidene)-1-*tert*-butyl-2-cyclohexylethylenediimine (2). 1-*tert*-Butyl-2-cyclohexylethylenediamine (1.95 g, 9.83 mmol), 3,5-di-*tert*-butylsalicylaldehyde (4.60 g, 19.6 mmol), and a few drops of aqueous formic acid were dissolved in 125 mL of methanol and heated to reflux for 2 h. Product isolation produced a yellow solid (3.14 g, 51% yield). Crystals suitable for X-ray analysis were grown by slow evaporation of pentane. Anal. Calcd for $C_{42}H_{66}N_2O_2$: C, 79.94; H, 10.54; N, 4.44. Found: C, 79.35; H, 10.43; N, 4.42. ^1H NMR (C_6D_6, 300 MHz): δ 14.45 (bs, OH), 14.41 (bs, OH), 8.15 (d, $J = 5.7$, 2H, CH═N), 7.60 (t, $J = 3.9$, 2H, Ph-H), 7.19 (t, $J = 4.5$, 2 H, Ph-H), 3.18 (bm, 1H), 3.061.68 (bd, $J = 1.8$, 1H), 1.68 (s, $J = 18$H, *t*-Bu H), 1.60−0.60 (m, 13H), 1.35 (s, 18H), 0.85 (s, 9H). $^{13}C\{^1H\}$ NMR (C_6D_6, 75 MHz): δ 166.68, 159.95, 140.36, 137.99, 127.67, 126.54, 126.4, 118.84, 118.73, 78.64, 75.54, 49.02, 47.37, 40.25, 35.91, 35.32, 34.65, 32.11, 31.27, 30.35, 30.21, 28.30, 26.88, 26.76, 26.29.

Synthesis of *N*,*N*′-Bis(3,5-di-*tert*-butylsalicylidene)-1-*tert*-butyl-2-methylethylenediimine (3). 1-*tert*-Butyl-2-methylethylenediamine (1.69 g, 13.0 mmol), 3,5-di-*tert*-butylsalicylaldehyde (6.06 g, 25.9 mmol), and a few drops of aqueous formic acid were dissolved in 125 mL of methanol and heated to reflux for 2 h. Product isolation produced a yellow solid (1.58 g, 22% yield). Anal. Calcd for $C_{37}H_{58}N_2O_2$: C, 78.92; H, 10.38; N, 4.98. Found: C, 78.90; H, 10.62; N, 4.99. ^1H NMR (C_6D_6, 300 MHz): δ 14.40 (bs, 2H), 7.99 (d, $J = 2.4$, 2H), 7.6 (d, $J = 2.4$ Hz, 1H), 7.58 (d, $J = 2.4$ Hz, 1H), 7.17 (d, $J = 2.4$, 1 H), 7.09 (d, $J = 2.4$ Hz, 1H), 3.62 (m, 1H), 1.68 (d, $J = 0.9$, 18H), 1.34 (d, $J = 2.4$, 18H), 0.86 (d, $J = 7.5$, 9H), 0.83 (s, 3H). $^{13}C\{^1H\}$ NMR (C_6D_6, 75 MHz): δ 167.01, 165.67, 159.89, 159.61, 140.27, 140.20, 137.88, 137.82, 127.61, 127.46, 126.63, 126.51, 118.96, 118.76, 83.70, 64.00, 35.91, 35.89, 35.10, 34.66, 32.12, 30.20, 30.14, 28.21, 22.72.

Synthesis of *N*,*N*′-Bis(3,5-di-*tert*-butylsalicylidene)-*meso*-1,2-diphenylethylenediimine (4). *meso*-1,2-Diphenylethylenediamine (0.300 g, 1.41 mmol), 3,5-di-*tert*-butylsalicylaldehyde (0.760 g, 3.24 mmol), and a few drops of aqueous formic acid were dissolved in 50 mL of methanol and heated to reflux for 8 h, cooled to room temperature, and then placed in a freezer for 2 h. Product isolation produced a yellow solid (0.7 g, 77% yield). ^1H NMR ($CDCl_3$, 300 MHz): δ 13.50 (s, OH, 2H), 8.25 (s, CH═N, 2H), 7.37 (d, $J = 2.6$, 2H), 7.31(m, 8H), 6.97 (d, $J = 2.3$, 2H), 4.80(s, 2H), 1.46 (s, 18H), 1.27 (s, 18H). $^{13}C\{^1H\}$ NMR ($CDCl_3$ 75 MHz): δ 166.03, 157.96, 140.00, 139.53, 136.46, 128.29, 127.59, 127.21, 126.31, 117.84, 79.66, 35.04, 34.08, 31.45, 29.41.

Synthesis of *N*,*N*′-Bis(3,5-di-*tert*-butylsalicylidene)-(±)-1,2-diphenylethylenediimine (5). (±)-1,2-Diphenylethylenediamine (0.512 g, 2.36 mmol), 3,5-di-*tert*-butylsalicylaldehyde (1.22 g, 5.21 mmol), and a few drops of aqueous formic acid were dissolved in 50 mL of methanol and heated to reflux for 8 h, cooled to room temperature, and then placed in a freezer for 2 h. Product isolation produced a yellow solid (1.29 g, 85% yield).

Synthesis of *N*,*N*′-Bis(3,5-di-*tert*-butylsalicylidene)-1-methylethylenediimine (6). 1-Methylethylenediamine (1.0 g, 13 mmol), 3,5-di-*tert*-butylsalicylaldehyde (6.31 g, 26.9 mmol), and a few drops of aqueous formic acid were dissolved in 50 mL of methanol and heated to reflux overnight. Product isolation produced a yellow solid (1.91 g, 28% yield). Anal. Calcd for $C_{33}H_{50}N_2O_2$: C, 78.19; H, 9.96; N, 5.53. Found: C, 77.88; H, 9.47; N, 5.31. ^1H NMR (C_6D_6, 300 MHz): δ 14.05 (bs, OH, 2H), 7.90(s, 1H, CH═N), 7.78 (s, 1H, CH═N), 7.55 (m, 2 H, Ph-H), 7.01 (d, $J = 2.7$, 1H, Ph-H), 6.97 (d, $J = 2.4$, 1H, Ph-H), 3.19 (bm, 3H), 1.63 (d, $J = 2.7$, 18H, *t*-Bu H), 1.03 (d, $J = 6.3$, 3H, Me-H). $^{13}C\{^1H\}$ NMR (C_6D_6, 75 MHz): δ 167.15, 167.11, 165.43, 158.17, 158.12, 139.57, 139.51, 136.41, 136.36, 126.45, 125.89, 125.81, 117.86, 117.83, 64.90, 64.17, 34.74, 33.59, 31.03, 29.10, 19.57.

General Synthesis of Cr^{III}(salen)Cl Complexes (1a-17a). Method A. The H_2salen ligand (1.0 equiv) and chromium(II) chloride (1.1 equiv) were dissolved in THF and stirred under argon at ambient temperature for 24 h. The reaction mixture then was exposed to air and stirred for an additional 24 h. After the reaction mixture was poured into diethyl ether, the organic layer was washed with aqueous saturated NH_4Cl (3×100 mL) and brine (3×100 mL) followed by drying with Na_2SO_4. After filtration to remove solid impurities and drying agent, solvent was removed in vacuo, yielding a dark brown powder.

Method B. Salicylaldimine (1.0 equiv) and KH (2.1 equiv) were dissolved in THF causing immediate gas evolution. After being stirred overnight, the cloudy white reaction mixture became a clear, light yellow solution. The potassium salt was transferred via cannula through a medium-porosity frit packed with Celite (to remove any solid particles and excess KH) to a flask containing $CrCl_3(THF)_3$ (1.1 equiv). Following an immediate color change of the chromium starting material from purple to reddish brown, the reaction mixture was stirred overnight at room temperature. The solvent was removed in vacuo, and the resulting solid was redissolved in dichloromethane. The reaction mixture was filtered to remove KCl, and solvent was removed in vacuo.

General Synthesis of Cr^{III}(salen)N_3 Complexes (1b-17b). The procedure previously reported by Jacobsen was followed.[18] The desired amount of Cr(salen)Cl complex was first dissolved in CH_3CN. In another Schlenk flask equipped with a pressure-equalizing addition funnel, 1 equiv of $AgClO_4$ was dissolved in an equal volume of CH_3CN. The Cr(salen)Cl solution was transferred via cannula into the addition funnel and added dropwise over approximately 20 min. Immediate precipitation of AgCl was observed, and the reaction was stirred overnight to ensure completion. Following this, the reaction mixture was filtered using a Büchner funnel (*note: perchlorate salts are potentially explosive and should not be used with fritted filters!*) and 3 equiv of NaN_3 was added, keeping exposure to air at a minimum. Sodium azide is only sparingly soluble in CH_3CN, and thus the reaction was allowed to stir for 24 h. The mixture was diluted with diethyl ether, the organic portion washed with water to remove $NaClO_4$ and excess NaN_3 and dried with Na_2SO_4, and the solvent removed in vacuo yielding a dark brown powder.

In Situ Infrared Monitoring of Epoxide Ring-Opening Reactions. A 50 mL beaker containing 10 mL of distilled toluene was initially cooled to the desired reaction temperature. Using an ASI ReactIR 1000 system equipped with an MCT detector and 30 bounce SiCOMP in situ probe, a single 64 scan infrared spectrum of solvent was utilized as a background. After this a jacketed 100 mL reaction cell that had previously been dried at 150 °C containing a magnetic stirbar was placed on the in situ probe and flushed with argon for 30 min. Once the cell was thoroughly flushed, a thermostated liquid circulating system containing a 50/50 ethylene glycol/water mixture was attached and the cell was cooled to the desired reaction temperature. An 18 mL toluene solution of ~300 mg of Cr(salen)N_3 complex was then added to the reaction flask. Once the system had come to equilibrium the spectrometer was started, collecting a 64 scan spectrum every minute for 4 h. After

(18) Leighton, J. L.; Jacobsen, E. N. *J. Org. Chem.* **1996**, *61*, 389−390.

Table 1. Crystallographic Data for Selected Salen Ligands and Chromium Salen Complexes

	1	2	7	1a	**2a**·H_2O	**11a**·**THF**·3THF
empirical formula	$C_{40}H_{64}N_2O_2$	$C_{42}H_{66}N_2O_2$	$C_{32}H_{48}N_2O_2$	$C_{40}H_{40}ClCrN_2O_2$	$C_{42}H_{66}ClCrN_2O_3$	$C_{52}H_{78}ClCrN_2O_6$
fw	604. 93	630.97	492.72	668.19	734.42	914.66
temp (K)	110(2)	110(2)	110(2)	110(2)	110(2)	110(2)
wavelength (Å)	0.710 73	0.710 73	0.710 73	0.710 73	0.710 73	0.710 73
cryst system	monoclinic	monoclinic	monoclinic	orthorhombic	monoclinic	monoclinic
space group	$P2_1/c$	$C2/c$	$P2_1/c$	$P2_12_12_1$	Pc	$P2_1/c$
a (Å)	11.052(9)	33.446(6)	6.145(3)	12.104(5)	6.5472(11)	16.253(16)
b (Å)	30.56(3)	12.858(2)	17.600(8)	14.875(6)	12.566(2)	26.26(3)
c (Å)	11.250(10)	18.768(3)	27.415(13)	22.512(8)	26.087(4)	11.705(12)
β (deg)	93.309(14)	91.156(6)	92.658(10)	90	96.418(3)	98.164(19)
cell vol (Å^3)	3793(6)	8069(2)	2962(2)	4053(3)	2132.8(6)	4945(9)
Z	4	8	4	4	2	4
D(calcd) (Mg/m^3)	1.059	1.039	1.105	1.643	1.144	1.227
abs coeff (mm^{-1})	0.064	0.062	0.068	0.57	0.367	0.335
obsd no. of reflcns	16 078	17 509	13 034	25 667	10 270	20 777
no. of unique reflcns [$I > 2\sigma(I)$]	5288	5819	4272	9317	5155	7143
R,[a] % [$I > 2\sigma(I)$]	0.0874	0.0647	0.0541	0.0644	0.0873	0.0644
R_w,[a] % [$I > 2\sigma(I)$]	0.1208	0.1478	0.0799	0.1160	0.1484	0.1109

[a] $R = \sum||F_o| - |F_c||/\sum|F_o|$. $R_w = \{[\sum w(F_o^2 - F_c^2)^2]/[\sum w(F_o^2)^2]\}^{1/2}$.

5 spectra, previously cooled epoxide was added and the reaction was monitored for changes in the ν(N═N) region of the infrared spectrum.

Copolymerization of Epoxides and CO_2. Cr(salen)X catalyst (50 mg) and *N*-methylimidazole were dissolved in 20 mL of neat epoxide. The solution was added via injection port into a 300 mL Parr autoclave at ambient temperature that was previously dried in vacuo at 80 °C overnight. The autoclave was charged with 500−600 psi of CO_2 and heated to 80 °C, producing a final pressure of ∼800 psi. After a period of 24 h, the autoclave was cooled to room temperature and vented in a fume hood. The polymer was extracted as a dichloromethane solution and dried under vacuum at 100 °C overnight.

The collected polycarbonate was analyzed by ^{1}H NMR, where the amount of ether linkages was determined by integrating the peaks corresponding to the methine protons of polyether at ∼3.45 ppm and polycarbonate at ∼4.6 ppm. Further analysis was done by infrared spectroscopy to identify monomeric *trans*-cyclohexyl carbonate with ν(C═O) at 1825 cm^{-1} and by ^{13}C NMR to determine the tacticity of the polymer formed. Molecular weight determinations (M_w and M_n) were carried out at the New Jersey Center for Biomaterials, Rutgers University. The GPC conditions are as follows: 20 mg of polymer was agitated with 2 mL THF (mobile phase). After 15 min, the sample is filtered with a 0.45 μm syringe filter followed by injection of 20 μL of filtrate using an autosampler. Separation occurred within 100 000 1000-Å PL gel columns (Polymer Laboratories) and monitored by a Waters 410 differential refractometer as detector. Data analysis was carried out using a Water Millenium 32 by comparing to polyethylene standards with known molecular weights at 483 000, 96 000, 30 300, 10 500, and 2470 g/mol.

High-Pressure in Situ Kinetic Measurements. High-pressure kinetic measurements were carried out using a stainless steel Parr autoclave modified with a SiComp window to allow for attenuated total reflectance spectroscopy using infrared radiation (ASI ReactiIR 1000 in situ probe). After the autoclave was dried in vacuo overnight at 80 °C, 10 mL of neat epoxide was loaded via the injection port. After the background solvent reached 80 °C, a single 128-scan background spectrum was collected. The desired catalyst and *N*-methylimidazole cocatalyst were dissolved in 10 mL of neat epoxide and injected into the autoclave followed by immediate charging with 50 bar CO_2 pressure. With a reaction temperature of 80 °C being maintained, a single 128-scan spectrum was collected every 3 min during a reaction period between 10 and 24 h. Profiles of the absorbance at 1750 cm^{-1} (polycarbonate) and ∼1825 cm^{-1} (cyclic carbonate) versus time were recorded after baseline correction. After cooling and venting in a fume hood, the polymer was extracted as a dichloromethane solution and dried under vacuum at 100 °C overnight.

X-ray Structural Studies. A Bausch and Lomb 10× microscope was used to identify suitable crystals from a representative sample of crystals from the same habit. The representative crystal was coated in a cryogenic protectant (i.e. mineral oil, paratone, or apezeon grease) and fixed to a glass fiber, which in turn was fashioned to a copper mounting pin. The mounted crystals were then placed in a cold nitrogen stream (Oxford) maintained at 110 K on a Bruker SMART 1000 three circle goniometer.[19]

The X-ray data were collected on a Bruker CCD diffractometer and covered more than a hemisphere of reciprocal space by a combination of three sets of exposures; each exposure set had a different φ angle for the crystal orientation, and each exposure covered 0.3° in ω. Crystal data and details on collection parameters are given in Table 1. The crystal-to-detector distance was 4.9 cm. Crystal decay was monitored by repeating the data collection for 50 initial frames at the end of the data set and analyzing the duplicate reflections and found to be negligible. The space group was determined on the basis of systematic absences and intensity statistics.[20] The structures were solved by direct methods and refined by full-matrix least squares on F^2. All non-H atoms were refined with anisotropic displacement parameters. All H atoms attached to C atoms were placed in idealized positions and refined using a riding model with aromatic C−H = 0.96 Å, methyl C−H = 0.98 Å, and fixed isotropic displacement parameters equal to 1.2 (1.5 for methyl H atoms) times the equivalent isotropic displacement parameter of the atom to which they were attached. The methyl groups were allowed to rotate about their local 3-fold axis during refinement.

Programs for all structures: data reduction, SAINTPLUS (Bruker20); structure solution, SHELXS-86 (Sheldrick[21]); structure

(19) *SMART 1000 CCD*; Bruker Analytical X-ray Systems: Madison, WI, 1999.
(20) *SAINT-Plus*, version 6.02; Bruker: Madison, WI, 1999.
(21) Sheldrick, G. *SHELXS-86: Program for Crystal Structure Solution*; Institut fur Anorganische Chemie der Uniseritat: Gottingen, Germany, 1986.

refinement, SHELXL-97 (Sheldrick[22]); molecular graphics and preparation of material for publication, SHELXTL-Plus version 5.0 (Bruker[23]). Space-filling models were obtained on a Unix-based system utilizing a Cerius graphics program.

Results and Discussion

One of our initial aims in examining the chiral chromium salen complex, (1*R*,2*R*)-(−)-[1,2-cyclohexanediamino-*N*,*N*′-bis(3,5-di-*tert*-butylsalicylidene)]chromium(III) chloride, as a catalyst for the copolymerization of the *meso* epoxide, cyclohexene oxide, and CO_2 was to exploit its intrinsic asymmetric ring-opening ability toward epoxides as described by Jacobsen.[11] That is, it was hoped that this catalyst would provide a polycarbonate with stereocontrol along the aliphatic backbone. Unfortunately, as observed in the carbonate region of the ^{13}C NMR spectrum, this chiral chromium catalyst afforded an atactic copolymer, much like that previously observed employing zinc phenoxide catalysts.[3a] This is supported by the elegant work of Nozaki and co-workers, who synthesized *syndio*- and *iso*-tetrad model carbonates and provided spectral assignments for the carbonate resonances.[24] In another study Nozaki and co-workers utilizing a catalyst derived from Et_2Zn and a chiral amino alcohol, (*S*)-α,α-diphenylpyrrolidine-2-ylmethanol, produced a highly isotactic copolymer from cyclohexene oxide and CO_2, which upon base hydrolysis produced a diol of >70% ee.[25] In closely related studies the enantioselective copolymerization of CO_2 and cyclohexene or cyclopentene oxide has similarly been achieved under milder conditions by Coates and co-workers using very active enantiomerically pure bis(oxazoline)-derived zinc complexes.[3d]

Although the chiral chromium salen complex was unsuccessful in the asymmetric copolymerization of carbon dioxide and cyclohexene oxide, it efficiently produced a copolymer with a low polydispersity and a high CO_2 content.[10] A detailed kinetic investigation of the reaction revealed that while the initiation step was likely second order in catalyst concentration, the subsequent enchainment steps were decidedly first order. This latter observation is consistent with the lack of enantioselective copolymerization noted since asymmetric ring-opening has been shown to involve a *second-order dependence* on catalyst concentration.[11] Our objective is to delineate the effects of altering the electronic and steric environments around the chromium center by changing the diimine backbone and/or phenoxide substituents of the salen ligand and observing the effects of these changes on the catalytic activity for poly(cyclohexylene)carbonate formation.

To assess the influence of substituents on the salen diimine backbone on catalytic activity, we have synthesized various diamines via the route described in eq 2. This procedure allows for the preparation of both symmetrically and unsymmetrically substituted diimines, i.e., $R_1 = R_2$ or $R_1 \neq R_2$. Crystal structures of three ligands prepared from condensation reactions of these diamines with 3,5-di-*tert*-butylsalicylaldehyde have been determined. Ligands **1** ($R_1 = R_2 =$ *t*-butyl) and **2** ($R_1 =$ cyclohexyl, $R_2 =$ *tert*-butyl) (Figures 1 and 2) show the substituted diimine groups to be in a trans orientation when the phenolic groups are adjacent to one another as seen in most metal salen structures. Ligand **7** ($R_1 = R_2 =$ H) (Figure 3) however orients its two half-salen units opposite one another such as it would exist when bound to two metal centers.[26]

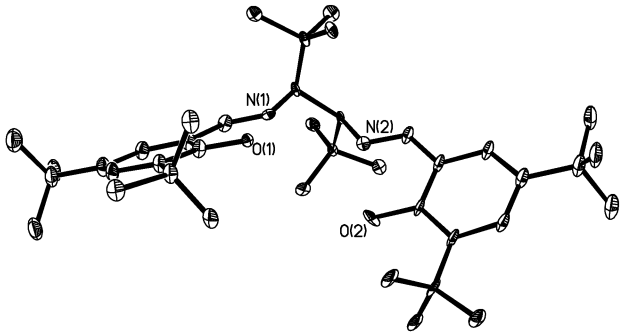

Figure 1. Thermal ellipsoid diagram of **1**, drawn at the 50% probability level.

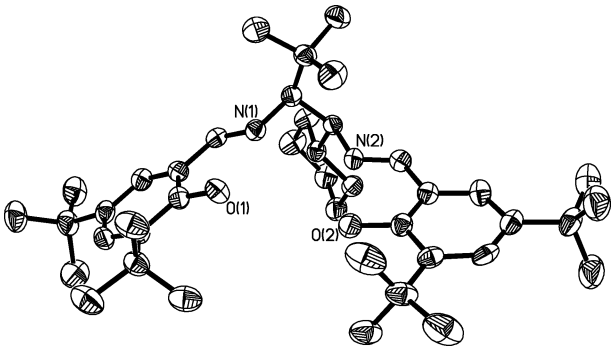

Figure 2. Thermal ellipsoid diagram of **2**, drawn at the 50% probability level.

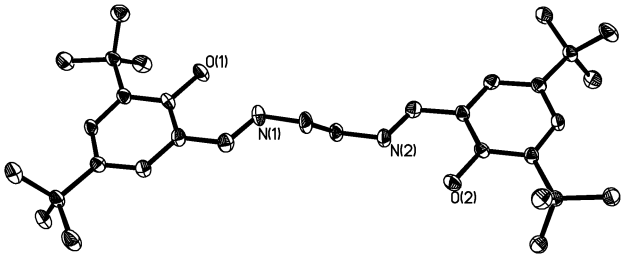

Figure 3. Thermal ellipsoid diagram of **7**, drawn at the 50% probability level.

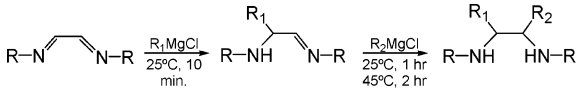

(2)

The solid-state structure of (salen)$Cr^{III}Cl$ (**1a**), where H_2-salen = **1**, is depicted in Figure 4, clearly illustrating the trans arrangement of the *tert*-butyl groups on the diimine backbone. This disposition of sterically encumbering sub-

(22) Sheldrick, G. *SHELXL-97: Program for Crystal Structure Refinement*; Institut fur Anorganische Chemie der Uniseritat: Gottingen, Germany, 1997.
(23) *SHELXTL*, version 5.0; Bruker: Madison, WI, 1999.
(24) Nakano, K.; Nozaki, K.; Hiyama, T. *Macromolecules* **2001**, *34*, 6325−6332.
(25) Nozaki, K.; Nakano, K.; Hiyama, T. *J. Am. Chem. Soc.* **1999**, *121*, 11008−11009.
(26) Darensbourg, D. J.; Draper, J. D. *Inorg. Chem.* **1998**, *37*, 5383−5386.

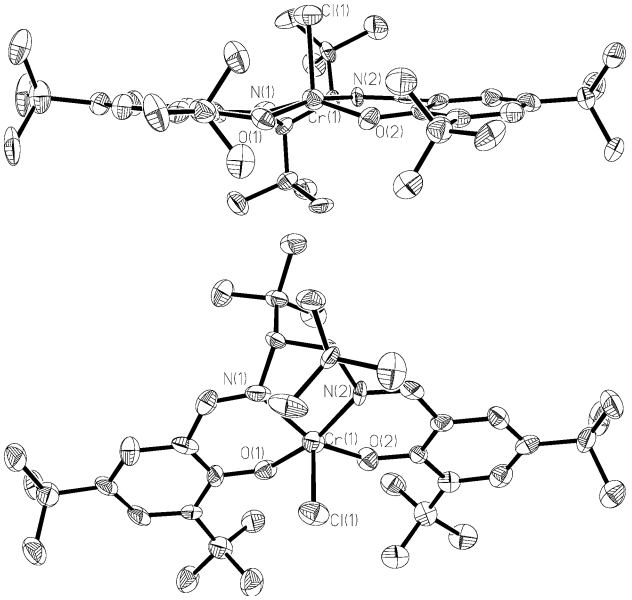

Figure 4. A 50% probability thermal ellipsoid plot of complex **1a**, showing both top and side views.

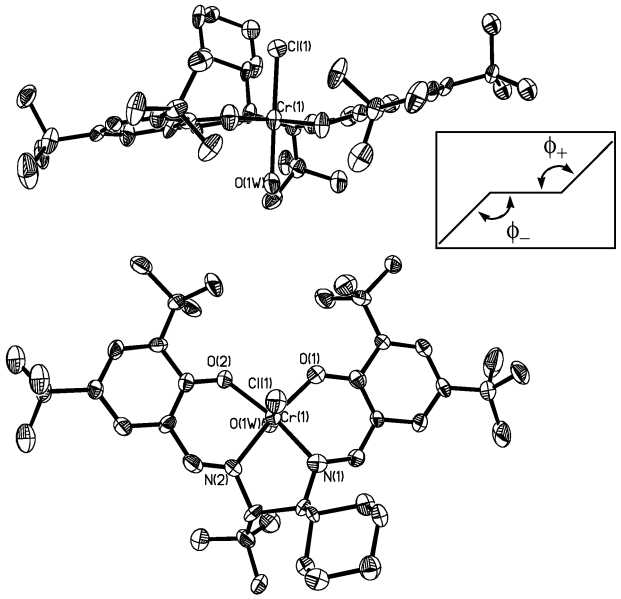

Figure 5. A 50% probability thermal ellipsoid plot of complex **2a**·H_2O, showing both top and side views.

stituents, coupled with the *tert*-butyl groups on the phenolic moieties, should severely hinder interactions adjacent to the anionic initiator by an approaching epoxide substrate. A similar situation is seen for the H_2salen = **2** chromium chloride derivative (complex **2a**·H_2O), where an axial water molecule is found coordinated to the metal center (Figure 5). Of significance, the Cr−Cl bond distance is lengthened in the six-coordinate complex **2a**·H_2O when compared with that observed in **1a**, 2.313(3) vs 2.239(3) Å, respectively. That is, axial ligation of the chromium salen complex leads to a destabilization of the trans Cr−Cl bond. Furthermore, unlike in complex **1a** where the ligand exhibits a planar coordination mode, the presence of an axial ligand results in a coordinated salen ligand which is folded with folding

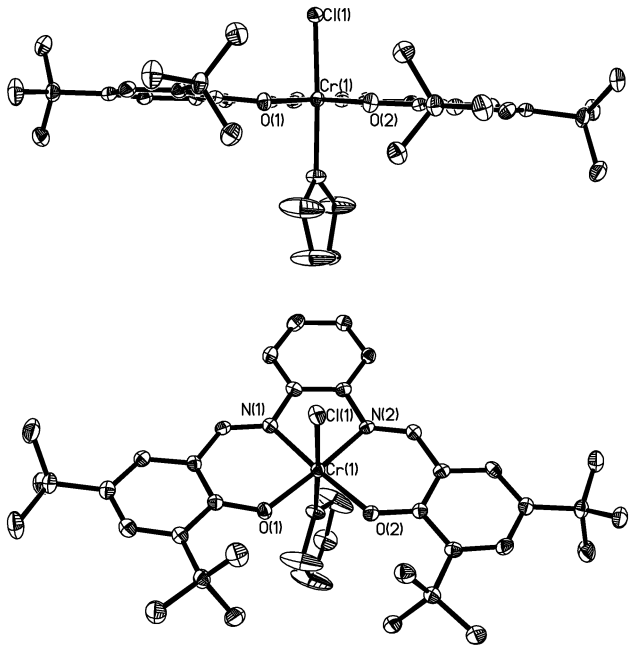

Figure 6. A 50% probability thermal ellipsoid plot of complex **11a·THF**, showing both top and side views.

angles (ϕ_+ and ϕ_-) of 162 and 169°.[27] On the other hand the *N*,*N*′-bis(3,5-di-*tert*-butylsalicylidene)-1,2-phenylenediimine derivative (**11a·THF**) with an axially bound THF ligand contains a near perfectly planar salen ligand (ϕ_+ and ϕ_- = 178 and 179°), which is consistent with extensive conjugation along the ligand framework (Figure 6).

A comprehensive list of copolymerization reactions of cyclohexene oxide and carbon dioxide is presented in Table 2. These reactions were performed under identical conditions (55 bar, 80 °C, 24 h) with a catalyst loading of less than 0.08 mol %. The processes were catalyzed by (salen)$Cr^{III}X$ (X = Cl or N_3) complexes in the presence of 2.25 equiv of *N*-methylimidazole as cocatalyst. The substituents on the salen ligand were varied over a wide range of steric and electronic properties as illustrated in Figure 7 and Table 2.

Upon careful examination of the catalytic activity of the various (salen)CrX complexes listed in Table 2, it is readily apparent that sterically encumbering substituents on the diimine backbone oriented perpendicular to the salen plane have a pronounced negative effect on copolymer production. The origin of this steric inhibition is presumed to be that it hinders the epoxide's interaction with the catalyst and subsequently its ring-opening. This is seen in the first four entries, where only a small quantity of copolymer is afforded with varying amounts of ether linkages (10−50%). For example, in complex **1a** the two *tert*-butyl groups render the metal barely accessible as illustrated by the space-filling models in Figure 8. This results in a TON of 20 mol of epoxide consumed/mol of Cr and a TOF of <1 h^{-1} with the copolymer having 48% carbonate linkages. Contrast this observation with the unsubstituted ethylene backbone derivative, complex **7a**, where a TON of 857 and a TOF of 35.7 h^{-1} with >99% carbonate linkages were observed. Similar

(27) Cavallo, L.; Jacobsen, H. *J. Org. Chem.* **2003**, *68*, 6202−6207.

Table 2. Copolymerization of Cyclohexene Oxide and CO_2 Catalyzed by (salen)CrX Complexes[a]

complex	R_1	R_2	R_3	R_4	X	TON[b]	TOF[c]	% carbonate[d]
1a	*tert*-butyl	*tert*-butyl	*tert*-butyl	*tert*-butyl	Cl	20	0.8	48
2a	*tert*-butyl	C_6H_{11}	*tert*-butyl	*tert*-butyl	Cl	36	1.5	61
3a	*tert*-butyl	CH_3	*tert*-butyl	*tert*-butyl	Cl	175	7.3	90
4a	*meso*-diphenyl		*tert*-butyl	*tert*-butyl	Cl	79	7.0	79
5a	(±)-diphenyl		*tert*-butyl	*tert*-butyl	Cl	1747	72.8	>99
5b	(±)-diphenyl		*tert*-butyl	*tert*-butyl	N_3	1907	79.5	>99
6a	CH_3	H	*tert*-butyl	*tert*-butyl	Cl	357	14.9	94
7a	H	H	*tert*-butyl	*tert*-butyl	Cl	857	35.7	99
7b	H	H	*tert*-butyl	*tert*-butyl	N_3	1126	46.9	>99
8a	H	H	H	H	Cl	270	11.2	92
9a	H	H	OCH_3	H	Cl	15	0.6	36
10a	H	H	OCH_3	*tert*-butyl	Cl	1360	56.7	>99
10b	H	H	OCH_3	*tert*-butyl	N_3	1505	62.7	>99
11a	$-C_4H_4-$		H	H	Cl	383	15.9	97
12a	$-C_4H_4-$		*tert*-butyl	*tert*-butyl	Cl	868	36.2	99
12b	$-C_4H_4-$		*tert*-butyl	*tert*-butyl	N_3	1030	42.9	>99
13a	$-C_4H_4-$		OCH_3	*tert*-butyl	Cl	1096	45.7	>99
13b	$-C_4H_4-$		OCH_3	*tert*-butyl	N_3	1581	65.9	>99
14a	$-C_4H_4-$		Cl	Cl	Cl	90	3.8	15
15a	*rac*-C_4H_8-		OCH_3	H	Cl	247	10.3	97
16a	(1*R*,2*R*)-C_4H_8-		*tert*-butyl	*tert*-butyl	Cl	851	35.5	99
16b	(1*R*,2*R*)-C_4H_8-		*tert*-butyl	*tert*-butyl	N_3	1197	49.9	>99
17a	(1*R*,2*R*)-C_4H_8-		OCH_3	*tert*-butyl	Cl	1575	65.6	96.0
17b	(1*R*,2*R*)-C_4H_8-		OCH_3	*tert*-butyl	N_3	1966	81.9	>99

[a] Each experiment was performed under 55 bar in CO_2, 20 mL of cyclohexene oxide, and 50 mg of catalyst in the presence of 2.25 equiv of *N*-MeIm over a 24 h reaction period. [b] mol of epoxide consumed/mol of Cr. [c] mol of epoxide consumed/(mol of Cr-h). [d] Estimated by ^{1}H NMR.

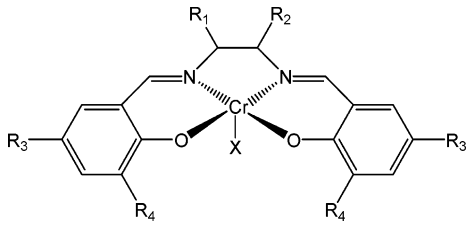

Figure 7. Generalized skeletal drawing of chromium(III) catalysts utilized in Table 2, where X = Cl (**a**) or N_3 (**b**).

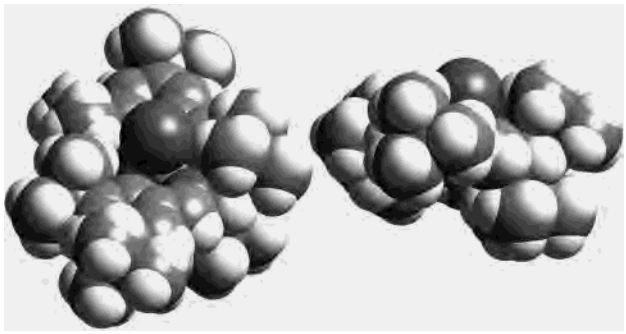

Figure 8. Space-filling models of complex **1a**.

somewhat less dramatic activity diminution is observed by employing slightly less sterically demanding diimine substituents than two *tert*-butyl groups as seen for catalysts **2a**−**3a**. Surprisingly, even relatively small substituents (R_1 = H, R_2 = Me, **6a**) decrease the activity by more than half when compared to **7a** ($R_1 = R_2$ = H). This effect is further explored through complexes **4a** and **5a**, where **4a** contains *meso* phenyl groups that would be in the same perpendicular orientation and **5a** contains phenyl groups oriented in a more parallel fashion as has previously been observed.[15] Again, as can be seen in Table 2, the rate of copolymerization for the *meso* complex (**4a**) is approximately a factor of 10 slower than that for the *racemic* complex (**5a**). These results further support the claim that sterics, not electronics, are the controlling factor along the diimine unit and the most active catalyst should have a less sterically crowded diimine backbone. As anticipated on the basis of steric arguments, the activities of complexes **7a**, **12a**, and **16a**, which contain ethylenediimine, cyclohexylenediimine, and phenylenediimine backbones, respectively, are almost identical. Similar activity trends are observed with azide metal complexes.

The *tert*-butyl groups on the phenolic ligands serve to greatly increase the solubility of the salen complexes. Indeed, some of the decrease in activity of complex **8a** ($R_3 = R_4$ = H) when compared with **7a** is due to a lack of solubility of the former chromium derivative. This is also the case for complex **9a** (R_3 = OMe, R_4 = H). However, by utilization of a combination of methoxy substituents *para* and a *tert*-butyl substituent *ortho* to the phenoxide group, both the solubility and electron-donating abilities of the salen ligand were efficiently maximized, with the ethyl (**10a**), phenyl (**13a**), and cyclohexyl (**17a**) diimine derivatives all yielding increases in the rate of copolymer production over their di-*tert*-butyl analogues. As previously observed, all of the diimine backbones exhibited similar rates of polymer production. Therefore, it has been demonstrated that increasing the electron-donating ability of the phenolate moieties has a significant positive effect on the rate of polymer formation, whereas a similar effect is not observed when modifying the diimine backbone.

As noted in Table 2 for copolymerization processes catalyzed by chromium salen derivatives differing only by the apical anionic ligand X (chloride or azide), the azide derivative is always the more active of the two. For example, the ethylenediimine backbone with $R_3 = R_4$ = *tert*-butyl the TOFs for Cl (**7a**) and N_3 (**7b**) are 35.7 and 46.9 h^{-1}, respectively. Whereas the steric and electronic factors on the salen ligands previously discussed are operative throughout

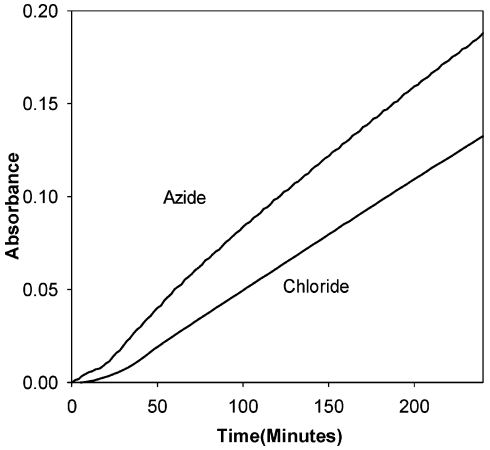

Figure 9. Peak traces of the ν(C═O) infrared band of the copolymer at 1750 cm^{-1} monitored by in situ infrared spectroscopy, showing the comparison between complexes **7a** and **7b**.

the copolymerization process, the role of the nucleophile (X) is only in the initial epoxide ring-opening step, i.e., the initiation step. Nevertheless, previous studies have shown that there is a significant initiation period before the maximum rate of catalysis is observed in the instance where X = Cl. On the other hand, in situ infrared spectroscopy shows that the initiation time for the azide complex is essentially zero, with polymer production beginning immediately (Figure 9).

At this point we wish to focus our attention on the initial epoxide ring-opening step using the ν_{N_3} vibrational mode in the azide catalyst (**7b**) as a probe for the process. Relevant to these efforts, Jacobsen and co-workers have previously shown that upon stirring a THF solution of Cr(salen)N_3, complex **16b**, and cyclohexene oxide overnight at ambient temperature, a shift in the ν_{N_3} absorption from 2054 to 2095 cm^{-1} was observed in the infrared spectrum. The ν_{N_3} vibration at 2054 cm^{-1} is that of the axially coordinated azide ligand in the THF adduct of the parent complex, (salen)-CrN_3·THF, and the shift to higher frequency is the result of azide ring-opening of the epoxide with concomitant formation of a chromium bound organic azide. These spectroscopic observations have been further confirmed by X-ray crystallographic characterization of both (salen)CrN_3·THF and the metal-bound alkoxide bearing an azide end group.[11b] This process has been demonstrated to occur via a bimetallic ring-opening process which is a key step in the mechanism proposed for the asymmetric ring-opening of epoxides.

Prior to this report it has not been shown that Cr(salen)N_3 derivatives in weakly coordinating solvents, such as hydrocarbons, display a ν_{N_3} vibrational mode at 2080 cm^{-1}, which corresponds to the five-coordinate chromium azide complex. By way of contrast, even in weakly coordinating solvents such as diethyl ether or methylene chloride the (salen)CrN_3 derivatives ν_{N_3} vibrational mode indicates interaction of the solvents with the metal center. Complex **7b** exhibits some solubility in hydrocarbon solvents, such as pentane and toluene. Preliminary experiments performed with **7b** in toluene at ambient temperature illustrated that both the binding and ring-opening of cyclohexene oxide can be

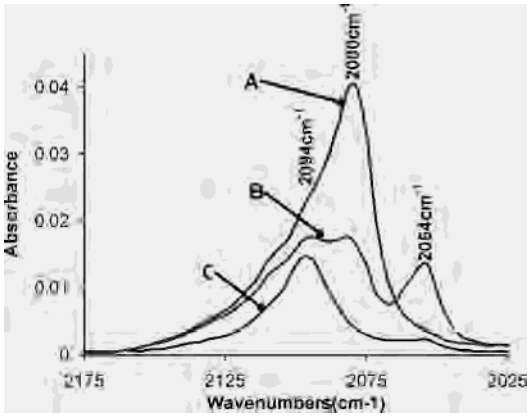

Figure 10. Overlay of spectra taken during the ring opening of cyclohexene oxide with complex **7b** at room temperature. Spectrum A was taken before epoxide addition, spectrum B was taken 30 s after epoxide addition, and spectrum C was taken 3 min after epoxide addition. The broadness of the band in (A) is reproducible and is thought to be due to weak solvent interactions.

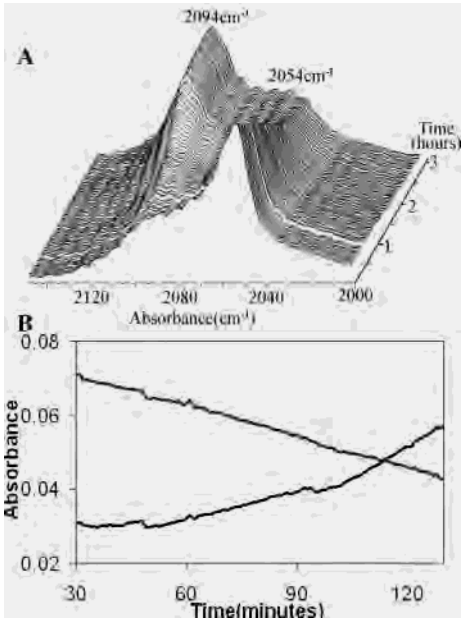

Figure 11. (A) 3-dimensional stack plot of the ring opening of cyclohexene oxide by complex **7b** at −10 °C and (B) the corresponding peak trace for both 2054 and 2094 cm^{-1}.

observed; however, the reaction goes to completion within 5 min of epoxide addition making kinetic analysis difficult (Figure 10). This rapid behavior was noted even when the epoxide concentration was limited to 1 equiv.

Experiments carried out at various temperatures showed that at −45 °C there was no binding of cyclohexene oxide to the metal center and hence no ring-opening of the epoxide was observed. Therefore, studies were performed at an intermediate temperature of −10 °C and in the presence of 25 equiv of cyclohexene oxide. Under these conditions, complete conversion of the (salen)CrN_3 complex occurs within 3 h (Figure 11). Attempted classical rate analysis of these data led to a second-order dependence of [catalyst] fitting the data slightly better than a first-order dependence (see Supporting Information).

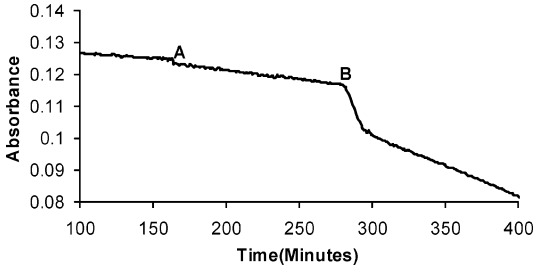

Figure 12. Reaction profile (disappearance of 2054 cm^{-1} ν_{N_3} band) for the ring opening of cyclohexene oxide with complex **7b**·*N*-methylimidazole at 25 °C. Epoxide was added at point A, and the temperature is increased to 60 °C at point B.

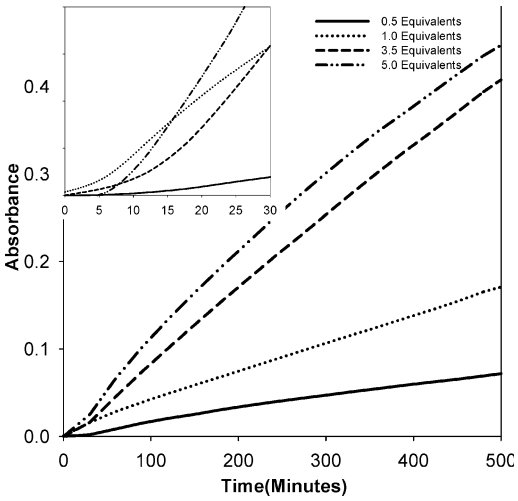

Figure 13. Initial effect on the addition of equivalents of *N*-methylimidazole to the rate of copolymerization for complex **7b**. Reaction was monitored by the formation of the polycarbonate ν_{CO_2} band at 1750 cm^{-1}.

In an analogous experiment involving complex **7b**, in the presence of 2.25 equiv of *N*-MeIm with *no* added epoxide, the ν_{N_3} stretching frequency was observed at 2054 cm^{-1} due to the formation of (salen)CrN_3·*N*-MeIm. Upon addition of 25 equiv of cyclohexene oxide to the above experiment, no shift in the ν_{N_3} mode was noted until the temperature was raised to 25 °C, where a very slow ring-opening reaction ensued. Even when the temperature was increased to 60 °C the rate of ring-opening of cyclohexene oxide by (salen)-CrN_3 was slow relative to that in the absence of the cocatalyst, *N*-MeIm (Figure 12).

Although the initiation step is greatly retarded in the presence of *N*-methylimidazole at ambient temperature, under the reaction conditions of the copolymerization process, 80 °C and an epoxide/*N*-MeIm ratio of 1000/1, this reaction is not significantly hindered. As illustrated by the in situ kinetic study presented in Figure 13 at low *N*-methylimidazole loadings, no significant initiation period is observed, and upon increase of the cocatalyst loading to 5 equiv, the initiation period is only slightly lengthened (vide infra).

We have shown the role of *N*-methylimidazole to be critical to copolymerization activity using (salen)CrX complexes as catalysts. Preliminary experiments involving **7a** as catalyst indicated that 5 equiv of *N*-MeIm was the optimum cocatalyst loading, with copolymer formation being inhibited at higher cocatalyst loadings.[10a] This was a key observation that led to the formulation of a plausible mechanism whereby the cocatalyst enhances the activity by binding to the metal center trans to the nucleophile (X or the growing polymer chain), thereby increasing its nucleophilicity. Recall that the Cr−Cl bond length in **1a** is elongated upon coordination of the axial ligand. However, an excess of cocatalyst severely inhibits epoxide binding and thus slows the bimetallic initiation step. Current reactivity studies using complexes **7a**,**b** provide only a slightly modified version of these earlier findings. That is, as indicated in Table 3 the initial increase in *N*-methylimidazole concentration substantially enhances copolymer formation, with a downturn in activity being observed at 30 equiv of cocatalyst. Concomitantly, at this high cocatalyst loading (30 equiv), there is a significant increase in polyether linkages as well as a dramatic decrease in the molecular weight of the copolymer. On the other hand, at 10 equiv, the TON increases dramatically, with only a slight reduction of carbonate linkages in the isolated copolymer.

Table 3. Copolymerization Activities of Complex **7a** at Different *N*-Methylimidazole Loadings

equiv of cocatalyst[a]	TON[b]	% carbonate linkages
0	82	80
1	317	97
2.25[c]	862	99
5	1141	97
10	1514	95
30[d]	749	87

[a] Copolymerization conditions: 50 mg of catalyst **7a** (0.04 mol %), 20 mL of cyclohexene oxide, 55 bar CO_2, 80 °C, 24 h. [b] Measured in mol of CHO consumed/mol of Cr. [c] A M_n of 8793, a M_w of 12 354, and a PDI of 1.4 were obtained. [d] A M_n of 2541, a M_w of 3133, and a PDI of 1.2 were obtained.

In efforts to further clarify the mechanistic aspects of the copolymerization process involving these (salen)CrX catalysts in the presence of *N*-methylimidazole as a cocatalyst, we have performed in situ infrared spectroscopic studies utilizing 2-(3,4-epoxycyclohexyl)ethyltrimethoxysilane (TMSO) as a comonomer. This epoxide has been shown to possess a similar reactivity for copolymer production as cyclohexene oxide but with the added advantage of the silyl tail allowing the copolymer to remain monophasic with carbon dioxide at high pressures and temperatures.[28] Through kinetic studies utilizing this epoxide, we have observed that the effect of increasing *N*-methylimidazole loading on the rate of copolymerization is 2-fold: the initiation time or the time required to reach the maximum rate of polymerization increases, and concomitantly the maximum rate once all active centers are initiated also increases (Figure 14).

It is worthwhile noting here parenthetically that while *N*-MeIm and DMAP have been used almost exclusively as cocatalysts for this type of chromium−nucleophile activation, their quantitative relative effects on activity have not been previously reported. Despite structural similarities, DMAP possesses significantly better donating ability as a result of the *para* orientation of the dimethylamino group. We have found that as with *N*-MeIm, a lengthening in initiation time

(28) Darensbourg, D. J.; Rodgers, J. R.; Fang, C. C. *Inorg. Chem.* **2003**, *42*, 4498−4500.

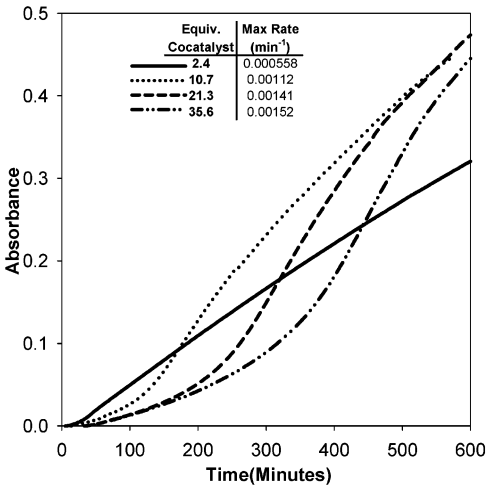

Figure 14. Peak traces of the ν(C═O) infrared band at 1750 cm^{-1} monitored by in situ infrared spectroscopy, showing the rate of polymerization for complex **7a** with different amounts of *N*-MeIm cocatalyst.

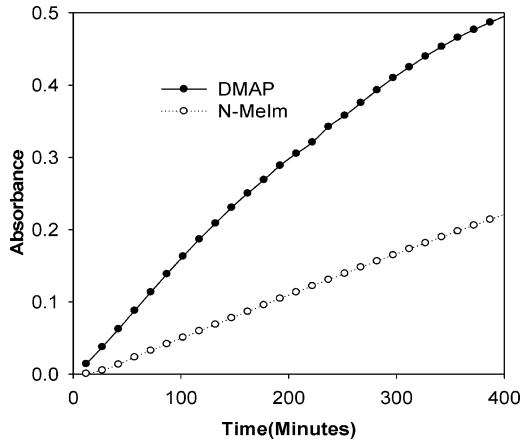

Figure 15. Formation of polycarbonate from TMSO and 55 bar CO_2 at 80 °C using **7a** with 2 equiv of DMAP or *N*-MeIm.

is observed upon increasing the DMAP concentration; however, propagation behavior differs dramatically. At identical loadings (2 equiv), DMAP has a much higher initial rate of polycarbonate formation compared to *N*-MeIm (Figure 15). However, beyond 2 equiv, polymer formation decreases with increasing DMAP concentration.

From these observations we conclude that while an increased cocatalyst loading inhibits initiation, chain propagation is enhanced. The synergism between these two steps most likely explains the anomalous activity data as well as earlier observations of complete inactivity at high *N*-methylimidazole loadings. In other words, if the reaction time is not sufficient, the catalyst would appear to be deceptively poisoned by excess amounts of *N*-methylimidazole. Further kinetic studies focused quantitatively on the influence of relative catalyst and *N*-methylimidazole loadings insofar as the propagation steps. Upon increase of the catalyst loading of **7a** or **7b** while a constant ratio (2.25:1) of cocatalyst: catalyst is maintained, a noninteger order (1.21, 1.38, respectively) with respect to [catalyst] was obtained. When the concentration of catalyst is kept constant and only the cocatalyst loading is varied, again a noninteger order (∼0.4) was found with respect to [cocatalyst], with a leveling off

Scheme 1

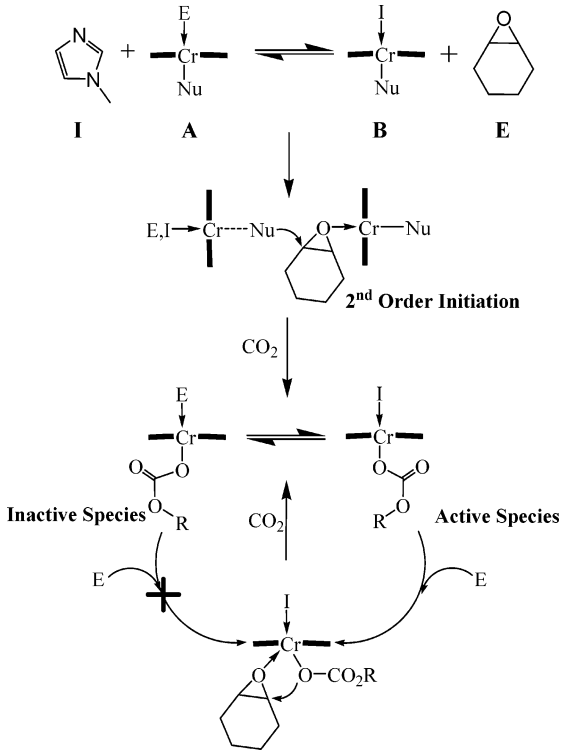

effect observed at higher *N*-methylimidazole loadings. Taken together, these findings suggest that an equilibrium exists between epoxide and cocatalyst binding trans to the propagating chain. The lack of activity when cocatalyst is absent suggests that the cocatalyst bound chromium complex is much more active than the corresponding derivative containing an axially bound epoxide. On the basis of this kinetic evidence, a more detailed mechanism can be proposed (Scheme 1). Initiation takes place via second-order activation whereby the cocatalyst activated nucleophile from one chromium center (**A**) ring opens an activated epoxide bound to a second metal center (**B**). The aforementioned azide studies suggest that in this instance this step may be significantly fast only requiring two molecules of **A** for epoxide ring opening and hence occur before in situ infrared monitoring begins. This would explain the lack of an observed initiation time for these complexes. In any event, for other less nucleophilic initiators the initiation step requires significant amounts of **A** and **B** to be present. While *N*-methylimidazole binding is favored, extremely high epoxide concentrations resulting from its use as a solvent make the overall formation of **A** competitive. Nevertheless, high cocatalyst loadings leads to a majority of the catalyst being present as **B**, hindering formation of the active species. Once the active species is formed, excess cocatalyst enhances the rate of propagation leading us to believe that an equilibrium is also maintained in the active species. However, this equilibrium varies from the previous one in that the reaction does not require significant amounts of species on both sides of the equilibrium and is enhanced by all of the catalyst being present as the *active species*. Therefore, the cocatalyst works

in both a hindering and supporting capacity in the initiation and propagation steps, respectively.

Concluding Remarks

The variation of ligand sterics/electronics as well as the relative loading of cocatalyst has dramatically improved the activities for epoxide/CO_2 copolymerization and, when compared to homogeneous zinc catalysts, represent some of the most active catalysts system studied by our group. When using *N*-methylimidazole as a cocatalyst, the proposed mechanism involves a bimetallic initiation step that is strongly inhibited by sterically bulky groups along the diimine backbone that protrude substantially out of the ligand plane. The use of an azide initiator increases activity substantially compared to chloride due its increased nucleophilicity and consequently shorter initiation times. Conversely, electron-donating groups in the ligand sphere, most effectively on the phenolate moieties, consistently result in higher turnover frequencies while maintaining high CO_2 incorporation in the isolated polymer. While this work supports our earlier claims with regards to the second order in [catalyst] initiation step and first-order mechanism for chain propagation, the role of cocatalyst has been clarified. In conclusion, since excess *N*-methylimidazole lengthens initiation time due to competition with epoxide at the site trans to the nucleophile, while simultaneously enhancing propagation, new cocatalyst systems with increased binding ability can be considered. As a result, studies conducted with diverse Lewis bases have already shown accelerated activities and are being actively pursued in our laboratories.[4c]

Acknowledgment. Financial support from the National Science Foundation (Grant CHE 02-34860) and the Robert A. Welch Foundation is greatly appreciated.

Supporting Information Available: Complete details for the crystallographic studies of compounds **1**, **1a**, **2**, **2a**·H_2O, **7**, and **11a**·**THF**·3THF (CIF), a description of the synthesis of compounds **6**−**17**, **1a**−**17a**, and **1b**−**17b**, and kinetic plots of cyclohexene oxide ring-opening reactions in the presence of (salen)CrN_3 (**7b**) in toluene solution. This material is available free of charge via the Internet at http://pubs.acs.org.

IC049182E